Oecologia (2000) 124:495–505 © Springer-Verlag 2000

U.G. Hacke · J.S. Sperry · B.E. Ewers · D.S. Ellsworth
K.V.R. Schäfer · R. Oren

Influence of soil porosity on water use in *Pinus taeda*

Received: 28 December 1999 / Accepted: 31 March 2000

Abstract We analyzed the hydraulic constraints imposed on water uptake from soils of different porosities in loblolly pine (*Pinus taeda* L.) by comparing genetically related and even-aged plantations growing in loam versus sand soil. Water use was evaluated relative to the maximum transpiration rate (E_{crit}) allowed by the soil-leaf continuum. We expected that trees on both soils would approach E_{crit} during drought. Trees in sand, however, should face greater drought limitation because of steeply declining hydraulic conductivity in sand at high soil water potential (Ψ_S). Transport considerations suggest that trees in sand should have higher root to leaf area ratios (A_R:A_L), less negative leaf xylem pressure (Ψ_L), and be more vulnerable to xylem cavitation than trees in loam. The A_R:A_L was greater in sand versus loam (9.8 vs 1.7, respectively). This adjustment maintained about 86% of the water extraction potential for both soils. Trees in sand were more deeply rooted (>1.9 m) than in loam (95% of roots <0.2 m), allowing them to shift water uptake to deeper layers during drought and avoid hydraulic failure. Midday Ψ_L was constant for days of high evaporative demand, but was less negative in sand (–1.6 MPa) versus loam (–2.1 MPa). Xylem was more vulnerable to cavitation in sand versus loam trees. Roots in both soils were more vulnerable than stems, and experienced the greatest predicted loss of conductivity during drought. Trees on both soils approached E_{crit} during drought, but at much higher Ψ_S in sand (<–0.4 MPa) than in loam (<–1.0 MPa). Results suggest considerable phenotypic plasticity in water use traits for *P. taeda* which are adaptive to differences in soil porosity.

Key words *Pinus taeda* · Xylem cavitation · Soil water transport · Root-shoot relations · Stomatal regulation

U.G. Hacke (✉) · J.S. Sperry
Department of Biology, University of Utah,
Salt Lake City, UT 84112, USA
e-mail: hacke@biology.utah.edu
Tel. +1-801-5850381, Fax +1-801-5814668

B.E. Ewers
Department of Forest Ecology and Management,
University of Wisconsin,
Madison, WI 53706, USA

K.V.R. Schäfer · R. Oren
Nicholas School of the Environment, Duke University,
Durham, NC 27708, USA

D.S. Ellsworth
Division of Environmental Biology,
Brookhaven National Laboratory,
Upton, NY 11973-5000, USA

Introduction

Plants are capable of growing in a wide range of soil textures ranging from coarse sand to heavy clay. These soils differ greatly in their hydraulic characteristics and present different challenges to plants trying to extract water from them (Bristow et al. 1984). At the same time, plants can differ considerably in their potential for water extraction, as determined by their cavitation resistance, root depth and density, and root-to-leaf ratio (Sperry et al. 1998). In this paper we investigated how the hydraulic traits of a single widespread species of pine (*Pinus taeda* L., loblolly pine) differed with respect to growth on a porous sand versus fine-textured loam soil. Specifically, we compared even-aged plantations of genetically similar stock on both soils to evaluate phenotypic rather than genetic adjustments to the different soil environments. *P. taeda* is widely planted across southeastern USA (over 20 million hectares) as well as in subtropical regions of South America and South Africa and hence frequently occurs on a wide variety of soil types.

Previous analyses of soil porosity and plant water use (e.g., Newman 1969; Bristow et al. 1984; Sperry et al. 1998) lead to a series of expectations for how plants might differ with respect to porosity so as to maintain water uptake. Here we summarize these predictions beginning with the soil and moving up the continuum to the leaves.

(1) Coarse soils lose more moisture and conductivity at higher water potentials than fine soils because of the

weaker capillary forces retaining water in the larger pore spaces. These differences are most pronounced across the coarse end of the soil texture spectrum from sand to loam (Campbell 1985). This suggests that plants growing in sandy soils require less negative water potential to exhaust their water supply than plants in a loam or finer soil. For the same reason, plants in sandy soil may become water-stressed at relatively high soil water potential. To the extent that plants in coarse soils have a greater need for accessing water at high water potential, they may also require deeper root systems in a drought-prone habitat than plants in fine soil to access soil at a high water potential.

(2) In addition to having deeper roots, plants in coarse soils should exhibit lower rates of water uptake per root surface area (rhizosphere flux density) than plants in fine soil to counter a potentially greater drop in rhizosphere hydraulic conductance during water uptake. There is a non-linear drop in soil water potential and conductivity as water funnels into a narrow root from the surrounding expanse of bulk soil (Cowan 1965; Newman 1969; Bristow et al. 1984). This can lead to critically low rhizosphere hydraulic conductance, especially in sandy soil where conductivity is very sensitive to soil water potential. Loss of hydraulic contact between parts of the root system and the soil can be minimized by developing a higher root to leaf area ratio (A_R:A_L) and/or by lowering the transpiration rate. Both features will reduce the rhizosphere flux density and are likely to be more pronounced in sandy soil.

(3) Once the water enters the plant xylem, it must rise to the leaves along a gradient in negative xylem pressure. This gradient depends on the hydraulic conductivity of the xylem per unit leaf area. Different xylem types differ substantially in their ability to sustain negative pressure without cavitation and subsequent loss of hydraulic conductivity of the xylem (Tyree and Sperry 1989). Cavitation resistance is correlated with the range of water potentials experienced by a plant, suggesting there are costs associated with having an overly resistant xylem. An adjustment of cavitation resistance to the amount of drought stress has been found among a wide variety of species (Sperry 1995; Davis et al. 1999; Hacke et al., in press) and also within populations of *Acer grandidentatum* (Alder et al. 1996). To the extent that plants growing in sandy soils operate under consistently higher water potentials, they may be more vulnerable to cavitation than plants in finer soils (Sperry et al. 1998).

(4) At the leaf level, plant water status is regulated by stomatal control of transpiration. Here, the effect of soil porosity may be on the sensitivity of stomata to declining soil water potential. Plants in sandy soils might be expected to show greater stomatal sensitivity to soil water potential than plants in fine soil as a result of the more limited range of water potential over which soil water is available.

In this paper, we tested if the water use and hydraulic properties of *P. taeda* growing on sand versus loam were adjusted to differences in soil porosity. Trees were similar in age and genetic background, and the sites were within the same region and experienced similar climatic conditions. However, the two soils provided a stark contrast in hydraulic properties. To compare water use at both sites we obtained data on numerous parameters, including transpiration, soil moisture and root profiles, A_R:A_L, cavitation resistance, plant hydraulic conductance, and plant water status through two growing seasons that included multiple droughts.

Data on plant and soil characteristics were used to parameterize a transport model (Sperry et al. 1998). This model integrated the measured plant and soil hydraulic properties to predict a transpiration rate (E) that could be validated against the measured E. The model also predicted the maximum hydraulically permissible transpiration rate (E_{crit}) above which water can no longer be transported to the leaves because of the loss of hydraulic conductance in the soil-plant continuum. The E_{crit} is a useful parameter because it is an estimate of the maximum potential for water extraction as defined by both soil and plant properties. We used the model to estimate how important the observed differences in water use between sites were for the maintenance of water uptake.

Materials and methods

Plant material and study sites

The loam site was a plantation of 15-year old *P. taeda* trees in the Duke Forest of central North Carolina (35°58' N, 79°8' W). It was in the same stand used for the free air CO_2 enrichment (FACE) project (Ellsworth 1999). The sand site was a 14- to 15-year-old plantation at the Southeast Tree Research and Education Site (SETRES) in the sandhills of south-central North Carolina (35° N 79° W; Albaugh et al. 1998; King et al. 1999). This facility is managed by the United States Forest Service.

The trees at both sites originated from the same nursery (Federal Paperboard in Lumberton, North Carolina) and were of the same central North Carolina provenance. Trees across both sites were related at the half-sib level based on analyses of amplified fragment length DNA polymorphisms, a DNA fingerprinting analysis (P. Keim, unpublished data).

At the loam site, soil texture was quantified as percentage sand, silt, and clay (Table 1). Six samples per site were taken at about 0.3 m depth and analyzed with the hydrometer method by the Utah State University Analytical Laboratory (Logan, Utah). At the sand site, we used silt and clay fractions averaged over 1.65 m depth as reported by Abrahamson et al. (1998) for the site. Both sites received only natural precipitation at an average annual rate of 1,210 mm for the sand site and 1,150 mm at the loam site.

Cavitation resistance and tracheid anatomy

We measured the relationship between xylem conductivity and water potential (a "vulnerability curve;" Tyree and Sperry 1989) using the centrifugal force technique to expose excised branch and root segments to known negative xylem pressures (Alder et al. 1997). Branch segments were from 1- and 2-year-old portions of prominent lateral branches in the mid to upper crown. Root segments were from three diameter classes: large (8.2–13.0 mm xylem diameter), medium (4.2–6.4 mm), and small (1.6–4.1 mm).

Table 1 Selected soil and plant parameters. Soil fractions are means of six measurements at the loam site (±SD) and taken from Abrahamson et al. (1998) for the sand site. Texture fractions and bulk densities were the basis for calculating the air entry potential (Ψ_e) and saturated hydraulic conductance (K_S). The b value for loam was taken from Oren et al. (1998a), and for sand was estimated from soil moisture data of Abrahamson et al. (1998). Bulk density was assumed to be 1.3 Mg m^{-3} (Campbell 1985) at the loam site, and taken from Abrahamson et al. (1998) for sand. Saturated leaf-specific hydraulic conductance of the whole plant (k_l*) was averaged from May (loam) or June (sand) data of 1997–1998 prior to drought. The leaf area index (*LAI*) range is May–August averaged for 1997–1998. Loam root area index (*RAI*) was based on fine root data from June 1997 (Matamala et al. 1998) and sand *RAI* was measured in winter 1998. The A_R:A_L was adjusted for *LAI* at the time of the *RAI* determinations

Parameter	Loam site	Sand site
Soil		
Clay fraction (%)	11.2	4.2
Silt fraction (%)	45.8	3.7
Sand fraction (%)	43.0	92.1
b	4.95	2.56
Ψ_e (kPa)	−1.77	−0.65
K_S (mol s^{-1} MPa^{-1} m^{-1})	18.8	107.8
Bulk density (Mg m^{-3})	1.3	1.42
Plant		
k_l* (mmol s^{-1} MPa^{-1} m^{-2})	0.65	1.07
Midday Ψ_L (MPa)	−2.31±0.22	−1.61±0.10
LAI	3.22-4.62	1.56–1.95
RAI	5.46	14.19
A_R:A_L	1.68	9.75

Roots were collected from the upper 0.40 m of soil. Six trees per site were sampled, with a minimum of one segment per type per tree. Trees were sampled between October 1997 and February 1998. Segments were 0.14 m long and were cut underwater from longer lengths collected in the field. Material was bagged in plastic for transport from field to laboratory.

In the laboratory, all segments were flushed with deionized and filtered (0.22 μm) water at about 40 kPa for 20 min to remove embolism. The initial (and maximum) hydraulic conductivity of the segments was measured as the flow rate of water through the segments divided by the pressure gradient (ca 50 kPa m^{-1}). Pressure was controlled by hydraulic head, and flow rate was measured gravimetrically. The tubing apparatus was bleached regularly to minimize microbial growth that could otherwise occlude the xylem.

Segments were mounted in a custom centrifuge rotor and spun with their ends immersed in water. The magnitude of the negative pressure in the segment was determined by the length of the segment and its angular velocity (Alder et al. 1997). Segments were spun for at least 3 min and then their hydraulic conductivity was remeasured. The process was repeated, spinning segments to progressively lower pressures until their hydraulic conductivity dropped to zero. Conductivity was stable after spinning indicating no refilling of cavitated tracheids during the flow measurement.

Vulnerability curves were plotted showing the percentage drop in hydraulic conductance versus xylem pressure (Fig. 2). To represent vulnerability curves by a single mean cavitation pressure, curves were converted to a non-cumulative frequency distribution of loss of conductance versus xylem pressure. The mean of this distribution was calculated using the midpoint of each pressure increment. The mean cavitation pressure will usually be similar to the xylem pressure that is associated with 50% loss of hydraulic conductance, with deviations depending on the asymmetry of the distribution.

We also measured tracheid diameters for comparison with mean cavitation pressure. Tracheid diameters were measured from a transverse section made at the middle of each segment. Diameters were determined in three radial sectors of the two outer growth rings at 120° intervals. A minimum of 100 tracheids were measured per segment. We used a light microscope interfaced with a bit pad (Donsanto Microplan II, Natick, Mass.) to trace lumen area and calculate the diameter of the equivalent circle. Tracheid diameters are reported as the hydraulic mean value. The hydraulic mean is the mean of the diameter distribution weighted in proportion to its theoretical contribution to hydraulic conductivity as postulated by the Hagen-Poiseuille law. Mathematically, the hydraulic mean tracheid diameter equals $\Sigma d^5/\Sigma d^4$ where d is tracheid diameter (Sperry and Ikeda 1997).

Ratio of root area to leaf area, leaf area index, and root area index

The ratio of root area to leaf area (A_R:A_L) was calculated from the ratio of root area index (*RAI*, root surface area per ground area) and leaf area index (*LAI*, projected leaf area per ground area).

At the sand site, *LAI* during 1997 and 1998 was calculated using allometric relationships with tree basal area derived from winter biomass harvests (Albaugh et al. 1998). Leaf area estimates for each tree were corrected for seasonality using the relative increase in *LAI* from winter to the sampling period as determined with a leaf area meter (*LAI*-2000; Li-Cor, Lincoln, Neb.) and litterfall. At the loam site, *LAI* was estimated from *LAI*-2000 measurements in September and corrected for seasonality using the model of Kinerson et al. (1974).

The *RAI* at the sand site was measured in January 1998 by excavating 1.9-m-deep, 1-m^2 pits, sorting roots into diameter classes (<1, 1–2, 2–5 mm) and depth classes (bounded by depths: 0, 0.15, 0.30, 0.50, 0.70, 0.90, 1.10, 1.30, 1.70, 1.90 m) and calculating area from total lengths in each class using the midpoint of the diameter class. We assumed the narrowest roots were 0.5 mm in diameter. A mean *RAI* was calculated from n=4 pits.

The *RAI* for the loam site was estimated as 5.46, a value derived from results of the FACE project for ambient CO_2 trees (Matamala et al. 1998). It was based on roots less than 1 mm diameter from five 0.2-m cores made in June 1997. The top 0.2 m accounted for 95% of the fine root biomass at this site, which has shallow soil (Matamala et al. 1998). This is consistent with a water budget for the site showing that >90% of the transpired water was coming from the top 0.35 m of soil (Oren et al. 1998a). To correct from area of small roots to total root area, we assumed the small roots contributed 70% of the total area, as was found by direct measurement for a comparable stand of *P. taeda* (Kinerson 1975).

Soil and leaf water potential

Soil water potential (Ψ_S) was estimated from water content measurements made with time-domain reflectometry probes. Vertical probes were installed in the shallow soil of the loam site to provide an integrated water content of the upper 30 cm (model CS615; Campbell Scientific, Logan, Utah). Horizontal probes (Theta probe; Delta-T Devices, Cambridge, UK) were installed at six depths (0.05, 0.15, 0.25, 0.5, 1, 2 m) in the deeper soils at the sand site. The 2-m probe was available only in the 1999 growing season. However, it averaged 0.002 cm^3 cm^{-3} higher water content than the 1-m probe with very little variation, and this value was used to back-calculate 2-m water contents for the 1998 and 1997 seasons. The conversion from water content to Ψ_S was given by Campbell (1985):

$$\Psi_S = \Psi_e(\theta/\theta_s)^{-b} \quad (1)$$

where θ is water content, θ_s is saturated water content, Ψ_e is the soil matric potential at air entry, and the exponent b is related to soil texture (larger for finer soils). Values for Ψ_e (Table 1) were calculated from sand, clay, and silt fractions according to Campbell (1985). A value for b at the loam site was available from previous work at the site (Oren et al. 1998a). b at the sand site was derived by fitting Eq. 1 to moisture release data from the site (Abrahamson et al. 1998).

Midday leaf water potential of single fascicles from the mid to upper canopy were measured with a pressure chamber for n=3 trees. Leaf water potential data for days of high vapor pressure deficit (D) during the two growing seasons showed no trend with Ψ_S at either site indicating that *P. taeda* exhibited "isohydric" behavior (Tardieu 1993) at these sites.

Midday transpiration

Transpiration was calculated from sap flux density measured with Granier-type sensors (Granier 1987). Sap flux density was averaged across eight trees at the sand site, and eight trees in three clusters at the loam site. Sap flux density was corrected to transpiration from estimates of sapwood area, radial trends of sap flux density, and *LAI* (Oren et al. 1998b; Ewers et al. 1999). Measurements of midday transpiration were averaged from half-hourly (or finer) readings made between 1200–1400 hours. Data were used for days from May–September 1997 and 1998 where the average D from 1200–1400 hours exceeded 1.5 kPa. The temperature and relative humidity for determining D were measured with thermistors and Vaisala sensors (HMP35C; Campbell Scientific).

Model application

The model (modified from Sperry et al. 1998) solved the relationship between steady state E (mmol s^{-1} m^{-2} leaf area) and the water potential difference driving flow in the soil-plant continuum:

$$E=k_l(\Psi_S-\Psi_L) \quad (2)$$

where k_l is the leaf-specific hydraulic conductance (in units of mmol s^{-1} MPa^{-1} m^{-2}), and Ψ_S is the bulk soil water potential. As E increases at a constant Ψ_S, Ψ becomes more negative in the continuum, and k_l decreases from xylem cavitation and soil drying in the rhizosphere. E reaches a maximum (E_{crit} and associated Ψ_{crit}) above which k_l goes to zero and hydraulic failure occurs.

The model divided the continuum into three components in series: rhizosphere (distance between bulk soil and root surface), root system, and shoot system (Fig. 1). Each component was assigned an initial "saturated" leaf-specific conductance (k_l*) representing the maximum conducting capacity prior to drought. The initial saturated rhizosphere k_l* (mmol s^{-1} MPa^{-1} m^{-2} of leaf area) was calculated from saturated soil conductivity (*KS*, mmol s^{-1} MPa^{-1} m^{-1}) assuming a cylindrical rhizosphere sheath of 8 mm thickness from bulk soil to root surface. The *KS* was determined from measured silt and clay fractions according to Campbell (1985; Table 1). The rhizosphere conductance on a root surface area basis was converted to a leaf area basis from estimates of A_R:A_L.

The initial saturated k_l* for root and shoot systems were assigned from in situ k_l [$=E/(\Psi_S-\Psi_L)$ measured at midday] averaged for May dates (loam site) or June dates (sand site – May data not available for both years) with midday (1200–1400 hours) D>1.5 kPa and prior to significant soil drying (Table 1). The root and shoot components were assumed to constitute 50% each of the total hydraulic resistance of the continuum as is typical of a wide variety of woody plants (Hellkvist et al. 1974; Saliendra and Meinzer 1989; Meinzer et al. 1992; Sperry and Pockman 1993; Yang and Tyree 1993; Mencuccini and Comstock 1997). Thus, k_l* of root and shoot was set to twice the measured early season k_l of the entire continuum.

For the shallow roots and soil of the loam site, the root system and rhizosphere was modeled as resistances in series (Fig. 1, left). To model the deeper roots at the sand site, the root system was divided into lateral and axial root components (Fig. 1, right). Lateral components serviced each of six soil layers centered on the six depths measured for water content (0.05–2 m). We scaled the component conductances proportional to upstream root area supplying each component, and inversely proportional to their relative lengths. Axial lengths were determined by relative depths of the midpoint of each soil layer. Lateral lengths were assumed to diminish linearly with depth from 1.5 m at 0.05 m to 0.5 m at 2 m.

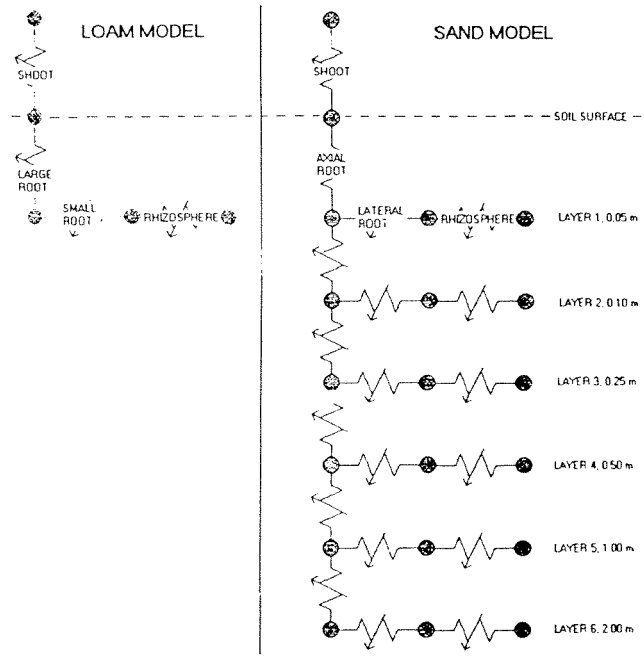

Fig. 1 Structure of the transport model. All resistances were variable because they were a function of water potential according to vulnerability curves of xylem and texture of soil. The loam model (*left*) consisted of three major resistances in series: shoot, root system, and rhizosphere. The root system was further divided into small and large roots to account for variation in cavitation resistance (Fig. 2). The sand model (*right*) consisted of six layers of roots servicing progressively deeper soil layers at depths corresponding to soil water content measurements. Each root layer consisted of lateral and axial root components that were assigned small and large root vulnerability curves, respectively

However, the model showed little difference if lateral root length was fixed at 1 m, suggesting little sensitivity to this parameter. The area- and length-based scaling assumptions allowed us to set the relative k_l* of each component. To convert these to the actual k_l* that accounted for 50% of the whole-plant resistance we used an iterative procedure. In this routine, the scaled k_l* of each component was set high, and then uniformly decremented until the root collar pressure corresponding to the measured E was half way between the field values of Ψ_S and Ψ_L. At this point, the k_l* of the entire root system was at the desired setting of twice the measured k_l of the whole plant.

Once the model was initialized with the appropriate k_l* values, it was used to predict seasonal changes in E_{crit} and Ψ_{crit} for comparison with corresponding values of midday E and Ψ_L through two growing seasons. For each date, the model calculated changes in k_l relative to k_l* based on changes in *LAI*, A_R:A_L, and Ψ. The model assumed that needle and xylem production during the growing season occurred proportionally so that k_l* was independent of the seasonal increase in *LAI* observed from May through August. However, as needles fell and *LAI* dropped in September, the model increased k_l* in inverse proportion to the drop in LAI. Similarly, root area was assumed to keep pace with leaf area production leading to constant A_R:A_L until September needle drop at which point A_R:A_L increased in inverse proportion to the decrease in *LAI*. We also determined the sensitivity of the model to A_R:A_L as discussed in relation to Fig. 7 (Results).

The Ψ-dependent decrease in k_l for the root and shoot components was assumed to result from xylem cavitation, and it was calculated from a Weibull function fit to vulnerability curve data:

$$k_l=k_l^*e^{-(\Psi/d)^c} \quad (3)$$

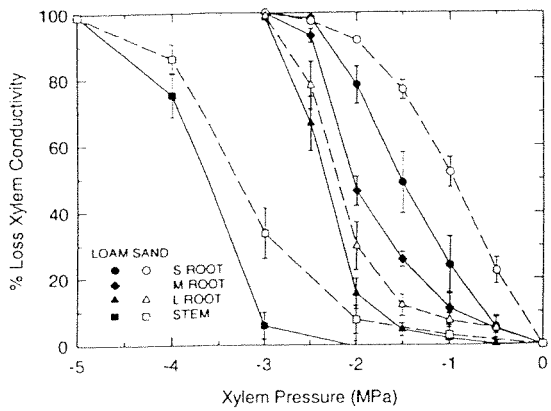

Fig. 2 Vulnerability curves showing the percentage loss of hydraulic conductivity in xylem vs xylem pressure for roots (*S* small 1.6–4.1 mm diameter; *M* medium 4.2–6.4 mm diameter; *L* large 8.2–13 mm diameter) and stems of sand (*open symbols*, *dashed lines*) vs loam (*solid symbols* and *lines*) trees. Standard errors are shown for means with n=6 segments from six trees per site

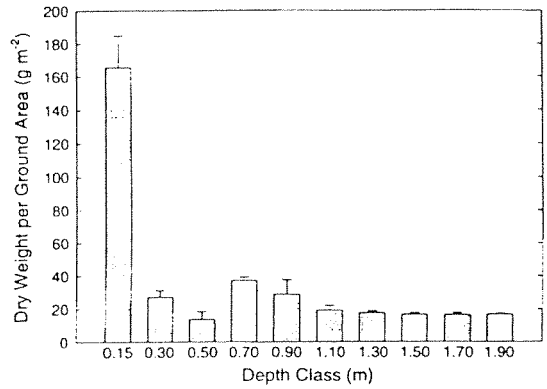

Fig. 3 Fine-root biomass vs depth at the sand site. Biomass means are shown with standard errors for n=4 soil pits. Fine roots were less than 1 mm in diameter. In contrast, 95% of fine roots at the loam site were in the top 0.2 m of soil (Matamala et al. 1998)

where d and c are curve-fitting parameters. As reported in the Results section, we found that the small roots were significantly more vulnerable to cavitation than larger roots (Fig. 2). To incorporate this variation in the loam site model, we assumed half of the root system conductance resided in roots represented by the small root vulnerability curve and the other half in roots represented by the large root curve (Fig. 1, left). A comparable assignation was made for the sand site where the lateral root components were given the small root vulnerability curve and the axial roots were given the large root curve (Fig. 1, right). The model assumed no reversal of cavitation with increasing Ψ following a drought. Thus, k_l*, d, and c in Eq. 3 were adjusted to the minimum Ψ experienced by root and shoot systems during the growing season.

The Ψ_S-dependent decrease in rhizosphere conductance was calculated as:

$$k_l = K_S X (\Psi_e / \Psi_S)^{(2+3/b)} \quad (4)$$

where X is a factor converting soil conductivity to leaf-specific rhizosphere conductance based on cylindrical geometry of the rhizosphere and the A_R:A_L ratio (Sperry et al. 1998), b and Ψ_e are soil parameters described earlier (Eq. 1, Table 1). Equation 4 was discretized for concentric rhizosphere shells as explained in Sperry et al. (1998). Unlike the k_l of the plant, the model assumed that decreases in k_l in the rhizosphere were reversible.

Results

Vulnerability curves and tracheid anatomy

At the loam site, cavitation in stem segments occurred between –3 and –5 MPa (Fig. 2, solid squares) with a mean cavitation pressure of –3.80±0.14 MPa (mean±SE, n=6). There was no difference between 1- and 2-year-old stems, so the data were pooled. Root xylem at the loam site was more vulnerable than stem xylem, cavitating at pressures between –0.5 and –3.0 MPa (Fig. 2). Although all root classes showed complete cavitation at –3 MPa, the smaller the root, the more vulnerable it was overall to cavitation (Fig. 2). Mean cavitation pressures of small and medium-sized roots (–1.50±0.12 and –1.85±0.04 MPa, respectively) were higher than large roots (–2.34±0.07 MPa, n=6, t-test P<0.05).

Trees at the sand site also had branches that were more resistant to cavitation than roots, and showed the same trend for greater vulnerability in narrower roots (Fig. 2, open symbols). However, these trees were more vulnerable to cavitation compared to those at the loam site. Mean cavitation pressure was higher in branch (–3.23±0.10 MPa, n=6) and small root (–1.05±0.06 MPa, n=6) categories compared to the loam site (P<0.05). There was no difference in the large root class (P>0.05), and medium-sized roots were not measured at the sand site.

The greater vulnerability of roots versus branches to cavitation was associated with roots having much larger tracheid diameters (hydraulic means=49.1±1.4 vs 17.2±1.1 μm, roots vs stems, respectively). Furthermore, the more vulnerable sand-site branches also had larger-diameter tracheids [18.7±0.37 (sand) vs 15.7±1.10 (loam), P<0.05]. Within roots, however, there was no correlation between tracheid diameter and cavitation resistance. Although small roots were more vulnerable than large roots, small roots had narrower tracheids (e.g., hydraulic means=49.2±2.2 vs 58.1±0.7 μm, respectively for sand trees).

Root to leaf area ratios (A_R:A_L)

The estimated A_R:A_L was nearly six times lower at the loam versus sand sites. Both the *RAI* and *LAI* contributed to this difference (Table 1). The measured *RAI* was much lower at the loam site (5.46, June 1997) than the sand site (14.19, January 1998). The difference was likely even greater because while the fine-root sampling for the loam site was essentially complete at 0.2 m depth (Matamala et al. 1998), the sampling at the sand site showed no sign of fine-root mass diminishing as the 1.9-m sampling depth was approached (Fig. 3). The *LAI*

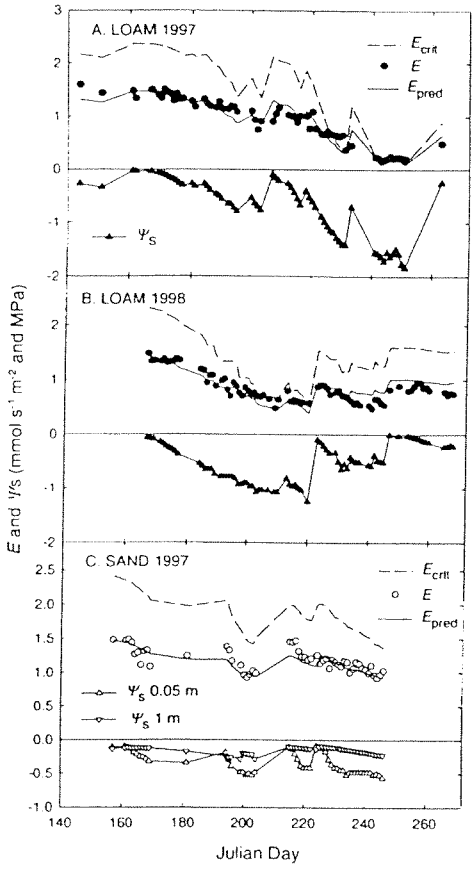

Fig. 4 Transpiration (E) and soil water potential (Ψ_S) vs Julian day for loam site 1997 (**A**), loam site 1998 (**B**), and sand site 1997 (**C**). Measured E (*circles*), modeled E (E_{pred} *line*), and modeled E_{crit} (*dashed line*) are shown for days with D>1.5 kPa. The Ψ_S (*triangles*) corresponds to 0.20 m depth for the loam site (**A**, **B**) vs 0.05 and 1 m depths at the sand site (**C**; *triangles* and *inverted triangles*, respectively)

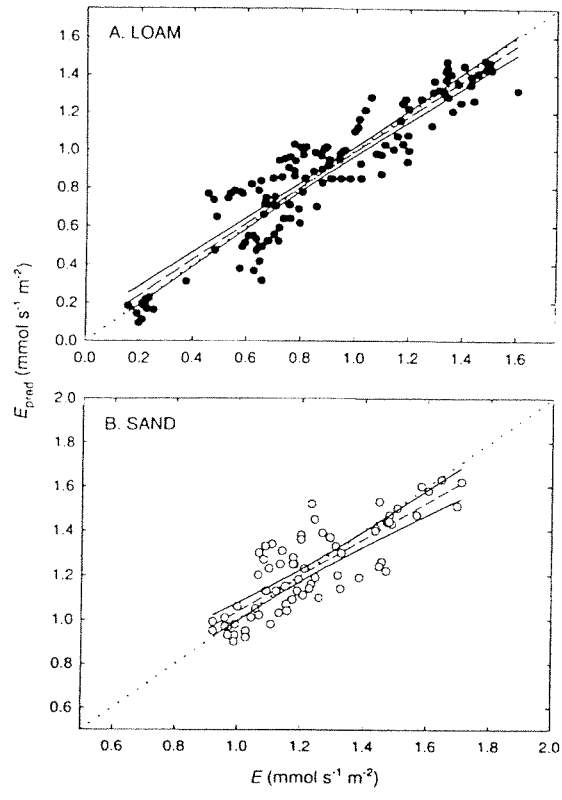

Fig. 5A, B Measured E vs modeled E (E_{pred}). **A** Loam site. Slope is 0.94 (r^2=0.85) and 95% confidence limits encompass the dotted 1:1 line. **B** Sand site. Slope is 0.82 (r^2=0.68) and 95% confidence limits encompass the 1:1 line over much of the measured E range

was higher at the loam (3.22–4.62 increase May through August) than sand sites (1.56–1.95 increase May through August). Based on estimated *LAI* at the time of the *RAI* measurement, the A_R:A_L was 1.68 at the loam site versus 9.75 at the sand site.

Seasonal patterns of transpiration (E) and water potential (Ψ)

Loam site

Figure 4 shows the seasonal course of E and Ψ_S for the 1997 (4A) and 1998 (4B) growing seasons at the loam site for days where D exceeded 1.5 kPa. Both growing seasons experienced significant drought with Ψ_S dropping to −1.8 MPa in 1997 and −1.1 MPa in 1998 (Fig. 4A,B, triangles). These droughts caused significant declines in E to less than 10% of maximum. Throughout the growing season, Ψ_L remained nearly constant at an average of −2.31±0.22 MPa (n=6 sampling dates) despite the large variation in Ψ_S.

The fit of the model was evaluated by comparing measured E (Fig. 4A,B, solid circles) with the E predicted (Fig. 4A,B, E_{pred} line) from the average midday Ψ_L. The E_{pred} closely tracked the measured E through both seasons with an r^2 of 0.85 (Fig. 5A). The 95% confidence limits on the E vs E_{pred} relationship encompassed the 1:1 line over the measured E range (Fig. 5A, regression slope=0.94). If the model assumed that the loss of root conductance during the drought was completely reversible following a drought it consistently overestimated E for post-drought values and the fit was not as good (data not shown).

The model predicted that trees closely approached but did not exceed E_{crit} as Ψ_S fell to −1 MPa or below during drought (Fig. 4A,B, compare E_{pred} line with dashed E_{crit} line). The measured E during these droughts remained centered on E_{pred}, and for the most part remained below E_{crit} or at most exceeded it because of normal random variation (Fig. 4A,B). Some of this variation may reflect non-steady-state conditions during the E measurement vs the steady-state model predictions of E and E_{crit}.

Sand site

Figure 4C shows the seasonal pattern of E and Ψ_S at the sand site for 1997 and D>1.5 kPa. Only partial data were

available for 1998 (shown only in Fig. 5B) owing to equipment failure during a drought period in July. The 1997 droughts roughly paralleled those at the loam site, and are evident from the drop in Ψ_S measured at 0.05 m (Fig. 4C, triangles). The droughts had a more subtle influence on Ψ_S at 1.0 m (Fig. 4C, inverted triangles). Ψ_S did not drop to the low values seen at the loam site despite similarly low rainfall. This probably reflected the inability of the trees to dry out the bulk soil much below –0.5 MPa owing to the large drop in water content and conductivity in the coarse sand soil (see Fig. 8 and below). There was no evidence from the continuous soil water content measurements of nocturnal hydraulic lift of water from deep to shallow soil (Richards and Caldwell 1989).

Droughts were associated with declines in E (Fig. 4C), but not of the magnitude seen at the loam site. The midday Ψ_L showed no trend with Ψ_S, and remained approximately constant at –1.62±0.10 MPa (n=5 sampling dates). This was significantly higher (P<0.05) than midday Ψ_L of –2.31 MPa at the loam site (Table 1). Figure 5B shows the relatively good fit (r^2=0.68) between modeled E_{pred} values (E_{pred} line) and the measured E (open circles). The 95% confidence limits on the E vs E_{pred} relationship over both growing seasons encompassed the 1:1 line over most of the measured E range (Fig. 5B, regression slope=0.81).

Although safety margins from E_{crit} diminished under drought conditions, E did not converge as closely on E_{crit} as in loam trees (Fig. 4). The relatively large safety margins and E under drought conditions was associated with a predicted shift in water uptake to deeper soil layers during drought (Fig. 8). On a day when Ψ_S was equal and high throughout the soil profile (Fig. 4C, first day shown), the model predicted relatively even water uptake with depth, with a shallow maximum in the upper meter (Fig. 8A, solid circles). In contrast, on a day when Ψ_S was below –0.5 MPa in the shallow soil layers (Fig. 4C, last day shown) water uptake was sharply reduced in the upper soil layers, and increased at depth (Fig. 8A, open circles). The shift to deeper roots was caused by a severe drop of hydraulic conductance in shallow soil layers owing to soil drying and root cavitation (Fig. 8B). The sharp reduction in water uptake from surface soil at only –0.5 MPa was due to soil conductivity being very sensitive to Ψ_S in the sandy soil, and the vulnerable xylem of the sand tree root system.

Comparison of water extraction between sites

To facilitate comparison in water use between sites, Fig. 6 shows E vs Ψ_S for a subset of the 1997 and 1998 data shown in Fig. 4 for monotonically declining Ψ_S. This eliminated variation in E associated with the lack of recovery in xylem conductivity when soil was rewetted following a drought. E is shown on a ground area rather than a leaf area basis to factor out the influence of variation in LAI on E. The dashed line is E_{crit}, the solid line is the predicted E, and the open symbols are measured E. The E_{crit}

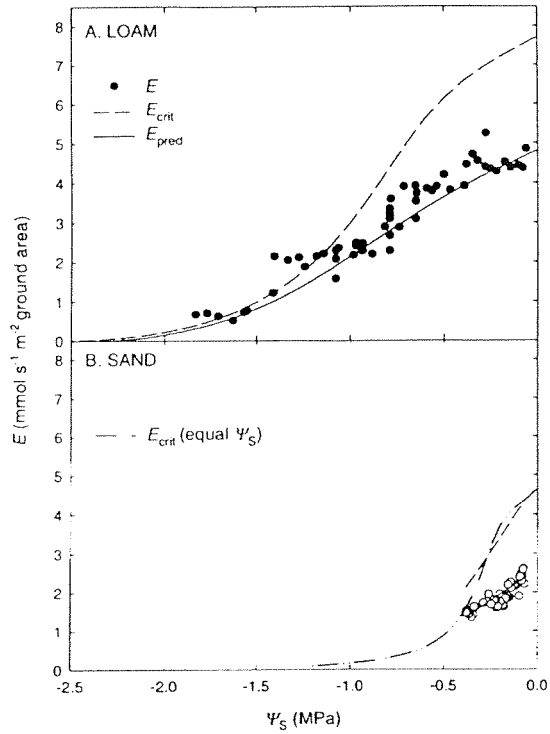

Fig. 6A, B Transpiration rate (per ground area) vs soil water potential (Ψ_S) for a monotonic decline of Ψ_S. Data extracted from the 1997–1998 growing seasons. **A** Loam site [*circles* measured E, *solid line* modeled E (E_{pred}) based on a midday average Ψ_L=–2.31 MPa, *dashed line* E_{crit}]. **B** Sand site. Symbols as in **A** (*dash-dotted line* E_{crit} assuming equal Ψ_S throughout the soil profile)

line for the sand site (Fig. 6B, dashed line) could not be extrapolated beyond the data because it depended on the variation in the Ψ_S profile with depth (the Ψ_S axis in Fig. 6B represents the mean for the profile). However, we also show E_{crit} for the sand site assuming equal Ψ_S in the profile (Fig. 6B, dash-dotted line) to enable direct comparison with the loam site.

At both sites, the convergence of E on E_{crit} under drought conditions is evident. A comparison of the E_{crit} curves in Fig. 6A and B shows that water use at the sand site was severely limited with respect to Ψ_S. At the loam site, E approached its hydraulic limit as Ψ_S fell below –1 MPa. At the sand site, E approached E_{crit} based on an equal Ψ_S profile (dash-dotted line) for Ψ_S lower than –0.4 MPa. For the actual Ψ_S profile where deep roots accessed soil at relatively high Ψ_S, the E_{crit} (dashed line) was somewhat higher during drought as discussed above. The model predicted that water use at the sand site was an "all or nothing" proposition with maximal uptake for Ψ_S >–0.25 MPa, and an abrupt decline to nearly negligible uptake for Ψ_S <–0.5 MPa. In contrast, E_{crit} at the loam site declined much more gradually with Ψ_S, approaching negligible values at Ψ_S <–2.0 MPa.

In addition to the narrow Ψ_S window predicted for water uptake from sand, the sand trees also showed much lower rhizosphere flux density (uptake rate per

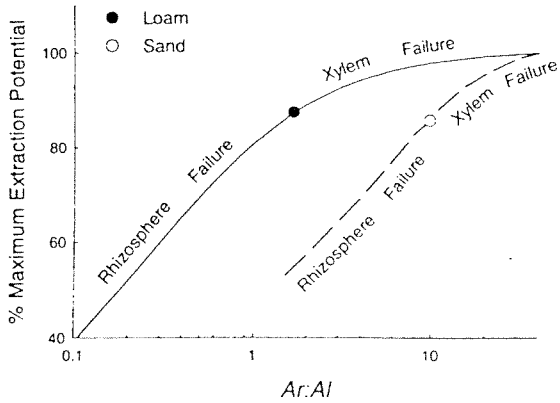

Fig. 7 Extraction potential vs A_R:A_L (*Ar:Al*) for loam (*solid line*) and sand (*dashed line*). Extraction potential is defined as area under the E_{crit} vs Ψ_S curve for the field range of Ψ_S (Fig. 6). Extraction potential is expressed as a percentage of the value at A_R:A_L=40. This value was chosen as a liberal estimate of the maximum likely physiological value for a woody plant. Symbols correspond to measured values of A_R:A_L for loam (*solid circle*) and sand (*open circle*)

unit root area). Based on the maximum E per ground area (Fig. 6) and the *RAI* (Table 1), maximum rhizosphere flux density averaged over the root profile at the sand site was 0.16 vs 0.88 mmol s^{-1} m^{-2} for the loam site. The lower rhizosphere flux density for sand trees was almost completely a result of their greater A_R:A_L because transpiration rates on a leaf-specific basis were similar between sites (Fig. 4). The decline in E with Ψ_S was much more sensitive to Ψ_S over the narrow range observed for the sand site (Ψ_S>–0.4 MPa), whereas there was no significant relationship (P>0.05) over the same range in loam trees. This is suggestive of greater stomatal sensitivity to Ψ_S at the sand vs loam sites.

The area under the E_{crit} vs Ψ_S curve in Fig. 6 was used to define the "extraction potential" from a drying soil. We used the model to determine the importance of the near sixfold increase in A_R:A_L between loam and sand sites on this extraction potential based on the measured range of Ψ_S at each site. For this comparison, we assumed an equal Ψ_S throughout the soil profile, so the results were independent of any variation in Ψ_S with depth.

As shown in Fig. 7, the extraction potential initially increased steeply with A_R:A_L before saturating. At low A_R:A_L values, extraction potential was limited by loss of hydraulic contact between the soil and parts of the root system, i.e., by loss of rhizosphere conductance. As A_R:A_L increased, the extraction potential saturated because cavitation in the xylem contributed progressively more to hydraulic failure such that further increases in A_R:A_L were ineffectual. The sand site required much higher A_R:A_L to saturate the extraction potential and shift hydraulic failure to the xylem (Fig. 7, compare dashed vs solid curves) as a result of the greater sensitivity of soil conductivity with Ψ_S for sand versus loam.

The actual A_R:A_L at each site (Fig. 7) was at a comparable point on the extraction curve, representing approximately 86% of the maximum extraction potential (at A_R:A_L=40, chosen as a very liberal maximum for woody plants). This result implies that the increase in A_R:A_L at the sand site was important for the maintenance of water uptake from this more hydraulically constraining soil. If the sand trees had had the low A_R:A_L of the loam trees, their extraction potential would have dropped by more than 50%.

Consistent with the relatively high extraction potential at both sites, the model predicted that hydraulic failure would occur in the xylem rather than the rhizosphere. Specifically, the failure would occur in the vulnerable root xylem under water-stressed conditions where E approached E_{crit} in the field. Substantial loss of root conductivity was also predicted by the model under drought conditions for both sites. No loss of conductivity was predicted in the shoot, owing to its much greater resistance to cavitation.

Discussion

The results showed substantial differences in the hydraulic properties of *P. taeda* trees growing on loam versus sand soil. The differences were consistent with expected adjustments to the very different hydraulic properties of the two soils. This implies considerable phenotypic plasticity in these traits given the similar age and genetic background of the trees.

Soil porosity and the operable Ψ range: associations with cavitation resistance and stomatal sensitivity

The effect of the different soils on the range of Ψ_S available for water uptake is evident from a comparison of the E_{crit} versus Ψ_S curve at the two sites (Fig. 6). Compared to the loam site where E_{crit} spanned a broad Ψ_S range down to –2 MPa (Fig. 6A, dashed line), the sand trees confronted an "all or nothing" situation with respect to water use with E_{crit} dropping sharply to a negligible value below –0.5 MPa.

Consistent with the narrower Ψ_S range for water uptake, trees in sand operated at higher Ψ_L (Table 1) and were more vulnerable to cavitation (Fig. 2). The shift to a greater vulnerability suggests there is some cost to having xylem that is more resistant to cavitation than necessary. A similar study on *P. taeda* found that greater cavitation resistance was associated with lower xylem conductivity per unit area (Ewers et al., in press). However, we found no such association in our study, and the cost of cavitation resistance remains elusive.

Sand trees also showed a greater stomatal sensitivity to Ψ_S as indicated by the greater decline in E for Ψ_S>–0.4 MPa at the sand versus loam sites (Fig. 6). According to the model, this greater sensitivity was required to avoid hydraulic failure. At both sites, the mechanism of stomatal regulation of E in response to drought was capable of responding not only to Ψ_S, but more importantly, to the significant reductions in hydraulic conductance of the continuum that accompanied the

drought. The mode of regulation at both sites was isohydric, meaning that midday Ψ_L remained constant despite variation in Ψ_S and in hydraulic conductance. Isohydric control of Ψ was also necessary in *Betula occidentalis* (Sperry and Pockman 1993; Saliendra et al. 1995), *Populus balsamifera* (Hacke and Sauter 1995), and *Sambucus nigra* (Vogt 1998) to prevent extensive cavitation. The simplest mechanism for isohydric regulation in the presence of variable Ψ_S and hydraulic conductance is a leaf-level feedback between stomatal conductance and the Ψ of sensory cells in the leaf, as has been demonstrated experimentally in trees (Saliendra et al. 1995; Fuchs and Livingston 1996) and shrubs (Comstock and Mencuccini 1998).

Soil porosity and rooting depth

The model indicated that the much deeper roots at the sand site (Fig. 3) were essential for maintaining at least some of the root system in water above –0.25 MPa, thereby insuring protection from hydraulic failure. For example, if sand trees had roots confined to the upper 20 cm of soil as at the loam site, the Ψ_S of their total rooting zone would have dropped below –0.5 MPa (Fig. 4C) and this would have required a more than 50% drop in E for these trees to avoid hydraulic failure (Fig. 6B). Consistent with this, the model predicted a shift to the use of deep water during surface drought (Fig. 8). Use of deep water buffered the trees from drought, as indicated by the more subtle declines in E and greater safety margin from E_{crit} at the sand site during the same weeks where E at the loam site was severely depressed and converged on E_{crit} (Fig. 4).

Independent studies of water use of sand-site trees are consistent with their predicted reliance on deep water. A water balance at the site indicated that over 30% of the transpired water comes from below 1 m during the growing season (Ewers et al., in press). A 3-year irrigation treatment at the sand site has shown only slight enhancement of growth (Albaugh et al. 1998; King et al. 1999; Ewers et al., in press). This is in agreement with the subtle drought response of non-irrigated trees (Fig. 4) and their access to relatively plentiful water at depth.

The results may seem contradictory in showing that the limitation on water uptake was greater for the sand trees (Fig. 6) when these trees showed relatively little drought response compared to loam trees (Fig. 4). However, as Figure 6 shows, trees in sand cannot experience much soil drying without having the bottom fall out of their water supply. To survive, they must escape even modest soil drying by having a deep root system.

Root-to-leaf area ratio, water extraction capability, and implications for nutrient interactions

Trees at the sand site also had a nearly sixfold higher A_R:A_L (Table 1) than loam trees. This had an important

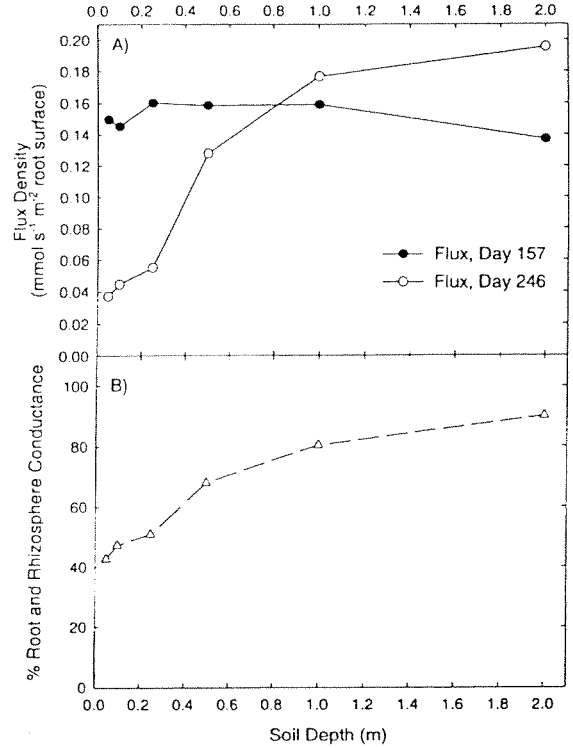

Fig. 8 **A** Flux density at the root surface for the six soil layers at the sand site (Fig. 1). Flux density is shown for first and last days of the 1997 data set (Fig. 4C), which represent maximum and minimum average Ψ_S over the period. **B** Hydraulic conductance at the sand site from bulk soil to root collar for each soil layer expressed as a percentage of the value on the first day. Data from the last day of the 1997 data set

influence on water uptake that was independent of the difference in rooting depth. As explained in the Introduction, A_R:A_L contributes to rhizosphere flux density and the consequent drop in rhizosphere conductance with water uptake. Too low an A_R:A_L can cause steep gradients in Ψ_S and lead to critical loss of hydraulic conductance in the rhizosphere. At both sites, A_R:A_L was high enough to avoid hydraulic failure in the rhizosphere and to approach maximum extraction potential (Fig. 7). Due to the much higher A_R:A_L at the sand site, the actual maximum rhizosphere flux density was over five times lower in the sand versus loam trees (0.16 vs 0.88 mmol s^{-1} m^{-2}).

It is noteworthy that both sites achieved a similar relative extraction potential (86%) as indicated in Fig. 7. From the standpoint of optimizing water uptake while minimizing root biomass, the 86% point is near where the cost of adding roots would begin to outweigh the diminishing returns for water extraction. Whether or not this is a general optimizing principle for the soil-plant continuum awaits further evaluation, particularly with respect to the role of roots in nutrient uptake.

As is often the case with sandy soils, the sand site is also nutrient poor compared to the loam site (King et al. 1999), and nutrient limitation can lead to some of the same adjustments that facilitate water uptake (e.g., high-

er A_R:A_L). Trees at the sand site that were given 5 years of fertilization (Albaugh et al. 1998) had an A_R:A_L of 4.6 versus 9.8 in non-fertilized trees (Ewers et al., in press). According to Fig. 7, this would reduce extraction to 66% of maximum. However, this was accompanied by an increase in cavitation resistance of the roots such that the extraction potential was actually only reduced to 77%. In trees given both irrigation and fertilization, A_R:A_L was 3.6 versus 9.8 in untreated plots and there was no change in cavitation resistance. This reduced extraction potential to 63%. However, this deficiency was not exposed because the irrigated trees were drought free (Ewers et al., in press). In both fertilized treatments, reduced extraction potential caused by nutrient addition implied greater vulnerability to drought-induced dieback versus non-fertilized trees. Thus, there was a significant antagonism between the shift in allocation triggered by fertilization versus the demands required for optimizing water uptake during drought. If irrigation were withheld from fertilized trees, our analysis predicts that their diminished water uptake capacity would result in severe water stress.

Applicability of the model

The model used to estimate E_{crit} gave a reasonable fit to the seasonal pattern of E (D>1.5 kPa) and Ψ data (Figs. 4, 5). This indicates that the prediction of water use during and after drought in plants requires information on the reductions in hydraulic conductance that occur as a result of both soil drying and xylem cavitation. Lack of such information would lead to overestimates of water use. By implication, the results suggest that changes in hydraulic conductance caused by processes not modeled, such as changes in radial conductance of roots or gaps between root and soil that were found in desert succulents (Nobel and North 1993) were less important to the overall continuum conductance than changes modeled in soil and xylem. In terms of model predictions, it is less important to identify *all* the causes of a change in conductance than it is to identify the *limiting* processes. Although the model can incorporate non-steady-state conditions (Sperry et al. 1998) that may further improve its predictions, the increased data requirements would make it more difficult to apply.

The weakest element of the model is the calculation of unsaturated soil conductivity which forms the basis of estimating rhizosphere conductance (Eq. 4). Unsaturated soil conductivity is a difficult parameter to measure directly, and in this study was estimated from soil texture parameters (Campbell 1985). The importance of Eq. 4 for model predictions increases as soils become coarser and changes in soil conductance become more important. Uncertainty in this parameter may underlie the somewhat poorer fit of the model to the sand site data (Fig. 5B).

Roots as a "hydraulic fuse"

The model and data together implicate root xylem as the weak link in the hydraulic continuum at both sites. This conclusion has also been reached in similar studies on woody species (Alder et al. 1996; Linton et al. 1998; Kolb and Sperry 1999). Under some circumstances roots may be acting as a hydraulic "fuse" analogous to the protective function of an electric fuse. Localizing hydraulic failure to the plant maximizes water extraction (Fig. 7). Further localizing it to the root system (especially the more vulnerable small roots; Fig. 2) minimizes replacement or refilling costs. Replacement of smaller roots can be achieved by regrowth, and refilling of cavitated root xylem following a drought would be enhanced by the high Ψ_S of surrounding wet soil. Though predicted to experience considerable cavitation in our study, the smaller loblolly roots may not have been able to refill after the drought, since assuming a lack of refilling produced a better model fit than otherwise. Lack of refilling may have resulted from senescence of severely cavitated roots (Seiler and Johnson 1988).

Acknowledgements Financial support was provided by NSF grant IBN-97-23464 to J.S. Sperry, and a Feodor-Lynen fellowship to U.G. Hacke from the Alexander von Humboldt Foundation. Support is acknowledged for the Duke Forest FACE by the US Department of Energy, Office of Health and Environmental Research, under DOE contract numbers DE-AC02-98CH10886 at Brookhaven National Laboratory and DE-FG05-95ER62083 at Duke University. Partial support from the US Department of Energy through the Office of Industrial Technologies, Forest Products Division is also gratefully acknowledged. Support for sap flux measurements at FACE and SETRES was obtained from the United States Forest Service (Southern Research Station), NSF grant BIR-9512333 to R. Oren, and the US Department of Energy through the University of Alabama's Southeast Regional Center of the National Institute for Global Environmental Change Cooperative Agreement No. DE-FC03-90ER61010.

References

Abrahamson DA, Dougherty PM, Zarnoch SJ (1998) Hydrological components of a young loblolly pine plantation on a sandy soil with estimates of water use and loss. Water Resour Res 34: 3503–3513

Albaugh TJ, Allen HL, Dougherty PM, Kress LW, King JS (1998) Leaf area and above and below-ground growth responses of loblolly pine to nutrient and water additions. For Sci 44: 317–327

Alder NN, Sperry JS, Pockman WT (1996) Root and stem xylem embolism, stomatal conductance, and leaf turgor in *Acer grandidentatum* populations along a soil moisture gradient. Oecologia 105:293–301

Alder NN, Pockman WT, Sperry JS, Nuismer S (1997) Use of centrifugal force in the study of xylem cavitation. J Exp Bot 48:665–674

Bristow KL, Campbell GS, Calissendorff C (1984) The effects of texture on the resistance to water movement within the rhizosphere. Soil Sci Soc Am J 42:657–659

Campbell GS (1985) Soil physics with basic; transport models for soil-plant systems. Elsevier, Amsterdam.

Comstock J, Mencuccini M (1998) Control of stomatal conductance by leaf water potential in *Hymenoclea salsola* (T. & G.), a desert subshrub. Plant Cell Environ 21:1029–1038

Cowan IR (1965) Transport of water in the soil-plant-atmosphere system. J Appl Ecol 2:221–239

Davis SD, Ewers FW, Wood J, Reeves JJ, Kolb KJ (1999) Differential susceptibility to xylem cavitation among three pairs of *Ceanothus* species in the Transverse Mountain Ranges of southern California. Ecosci 6:180–186

Ellsworth DS (1999) CO_2 enrichment in a maturing pine forest: are CO_2 exchange and water status in the canopy affected? Plant Cell Environ 22:461–472

Ewers BE, Oren R, Albaugh TJ, Dougherty PM (1999) Carry-over effects of water and nutrient supply on water use of *Pinus taeda*. Ecol Appl 9:513–525

Ewers BE, Oren R, Sperry JS (in press) Influence of nutrient versus water supply on hydraulic architecture and water balance in *Pinus taeda*. Plant Cell Environ

Fuchs EE, Livingston NJ (1996) Hydraulic control of stomatal conductance in Douglas fir [*Pseudotsuga menziesii* (Mirb.) Franco] and alder [*Alnus rubra* (Bong)] seedlings. Plant Cell Environ 19:1091–1098

Granier A (1987) Evaluation of transpiration in a Douglas-fir stand by means of sap flow measurements. Tree Physiol 3: 309–320

Hacke U, Sauter JJ (1995) Vulnerability of xylem to embolism in relation to leaf water potential and stomatal conductance in *Fagus sylvatica* f. *purpurea* and *Populus balsamifera*. J Exp Bot 46:1177–1183

Hacke UG, Sperry JS, Pittermann J (in press) Drought experience and cavitation resistance in six shrubs from the Great Basin, Utah. Basic Appl Ecol

Hellkvist J, Richards GP, Jarvis PG (1974) Vertical gradients of water potential and tissue water relations in Sitka spruce trees measured with the pressure chamber. J Appl Ecol 7:637–667

Kinerson RS (1975) Relationships between plant surface area and respiration in loblolly pine. J Appl Ecol 12:965–971

Kinerson RS, Higginbotham RC, Chapman RC (1974) The dynamics of foliage distribution within a forest canopy. J Appl Ecol 11:347–353

King JS, Albaugh TJ, Allen HL, Kress LW (1999) Stand-level allometry in *Pinus taeda* as affected by irrigation and fertilization. Tree Physiol 19:769–778

Kolb KJ, Sperry JS (1999) Transport constraints on water use by the Great Basin shrub, *Artemisia tridentata*. Plant Cell Environ 22:925–936

Linton MJ, Sperry JS, Williams DG (1998) Limits to water transport in *Juniperus osteosperma* and *Pinus edulis*: implications for drought tolerance and regulation of transpiration. Funct Ecol 12:906–911

Matamala R, Gallardo A, Schlesinger WH (1998) Fine root biomass, root respiration and phosphatase activity in a temperate forest ecosystem: effects of elevated atmospheric CO_2, FACTS-I experiment (abstract). GCTE-LUCC Open Science Conference on Global Change, Barcelona, Spain

Meinzer FC, Goldstein G, Neufeld HS, Grantz DA (1992) Hydraulic architecture of sugarcane in relation to patterns of water use during development. Plant Cell Environ 15:471–477

Mencuccini M, Comstock JC (1997) Vulnerability to cavitation in populations of two desert species, *Hymenoclea salsola* and *Ambrosia dumosa*, from different climatic regions. J Exp Bot 48:1323–1334

Newman EI (1969) Resistance to water flow in soil and plant. I. Soil resistance in relation to amounts of root: theoretical estimates. J Appl Ecol 6:1–12

Nobel PS, North GB (1993) Rectifier-like behaviour of root-soil systems: new insights from desert succulents. In: Smith JAC, Griffiths H (eds) Water Deficits. Bios, Oxford, pp 163–176

Oren R, Ewers BE, Todd P, Phillips N, Katul G (1998a) Water balance delineates the soil layer in which moisture affects canopy conductance. Ecol Appl 8:990–1002

Oren R, Phillips G, Katul G, Ewers BE, Pataki DE (1998b) Scaling xylem sap flux and soil water balance and calculating variance: a method for partitioning water flux in forests. Ann Sci For 55:191–216

Richards JH, Caldwell MM (1989) Hydraulic lift: water efflux from upper roots improves effectiveness of water uptake by deep roots. Oecologia 79:1–5

Saliendra NZ, Meinzer FC (1989) Relationship between root/soil hydraulic properties and stomatal behavior in sugarcane. Aust J Plant Physiol 16:241–250

Saliendra NZ, Sperry JS, Comstock JP (1995) Influence of leaf water status on stomatal response to humidity, hydraulic conductance, and soil drought in *Betula occidentalis*. Planta 196:357–366

Seiler JR, Johnson JD (1988) Physiological and morphological responses of three half-sib families of loblolly pine to water-stress conditioning. For Sci 34:487–495

Sperry JS (1995) Limitations of stem water transport and their consequences. In: Gartner B (ed) Plant stems: physiology and functional morphology. Academic Press, San Diego, pp 105–124

Sperry JS, Ikeda T (1997) Xylem cavitation in roots and stems of Douglas-fir and white fir. Tree Physiol 17:275–280

Sperry JS, Pockman WT (1993) Limitation of transpiration by hydraulic conductance and xylem cavitation in *Betula occidentalis*. Plant Cell Environ 16:279–288

Sperry JS, Adler FR, Campbell GS, Comstock J (1998) Limitation of plant water use by rhizosphere and xylem conductance: results from a model. Plant Cell Environ 21:347–359

Tardieu F (1993) Will increases in our understanding of soil-root relations and root signaling substantially alter water flux models? Phil Trans R Soc Lond B 341:57–66

Tyree MT, Sperry JS (1989) Vulnerability of xylem to cavitation and embolism. Annu Rev Plant Physiol Mol Biol 40:19–38

Vogt UK (1998) Strukturell-funktionelle Koordination von Wasserleitung und Transpiration als Grundlage des hydro-oekologischen Konstitutionstyps. PhD thesis, University of Duesseldorf

Yang S, Tyree MT (1993) Hydraulic resistance in *Acer saccharum* shoots and its influence on leaf water potential and transpiration. Tree Physiol 12:231–242